The Northern-Cross Fast Radio Burst project V.
Search for transient radio emission from Galactic magnetars

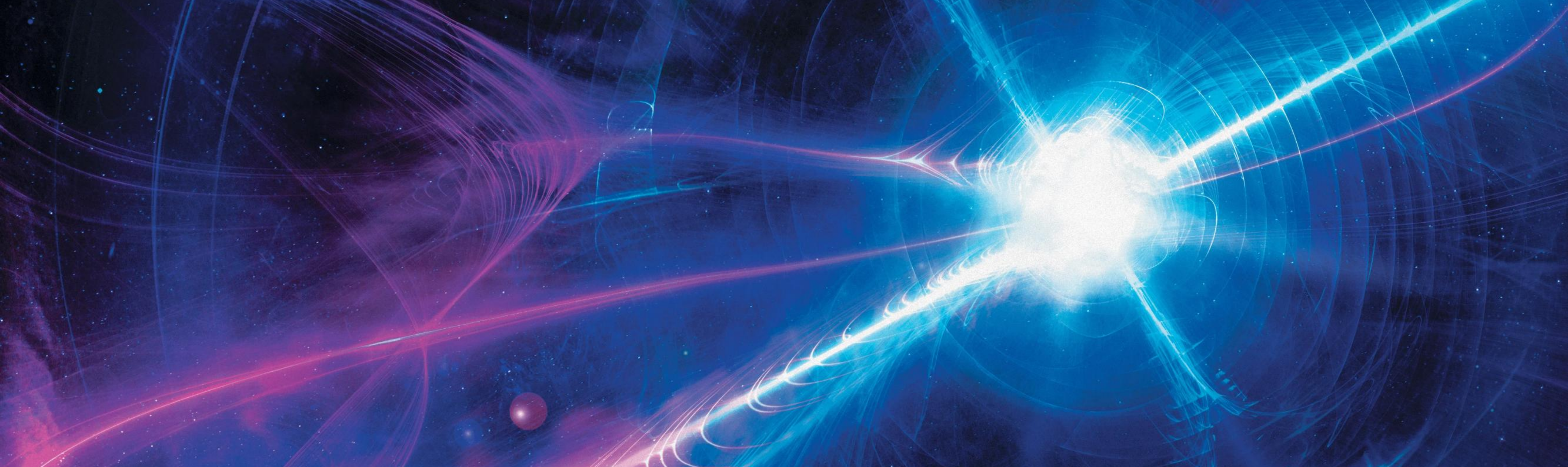

Andrea Geminardi

P. Esposito, M. Pilia,
G. Bernardi, D. Pelliciari,
Northern-Cross collaboration

UNIVERSITY OF TRENTO

PhD SST
Space Science and Technology

IUSS
Scuola Universitaria Superiore Pavia

INAF
ISTITUTO NAZIONALE DI ASTROFISICA

Finanziato dall'Unione europea
NextGenerationEU

Northern Cross

T-shaped transit radio telescope → $\sim 30000\ \mathrm{m}^2$ collecting area

$\tau_S = 138\ \mu s$

$B = 14.8\ \mathrm{MHz}$

$\nu_C = 408\ \mathrm{MHz}$

Currently under refurbishment

16 out of 64 N-S cylinders

Northern Cross

T-shaped transit radio telescope → $\sim 30000\ \mathrm{m}^2$ collecting area

↓

$\tau_S = 138\ \mu s$

$B = 14.8\ \mathrm{MHz}$

$\nu_C = 408\ \mathrm{MHz}$

↓

Currently under refurbishment

↓

16 out of 64 N-S cylinders

Few degrees field-of-view

RMS sensitivity $\sim$1 Jy

Primary beam attenuation

Locatelli et al. 2020

Geminardi et al. 2025 (submitted)

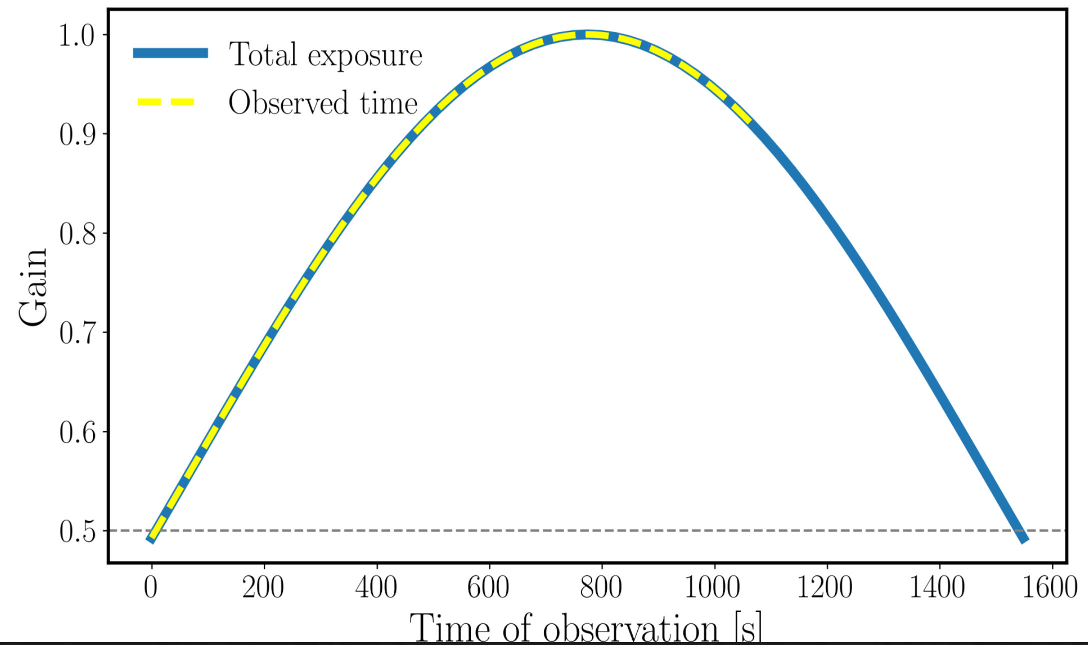

Detection pipeline

Geminardi et al. 2025 (submitted)

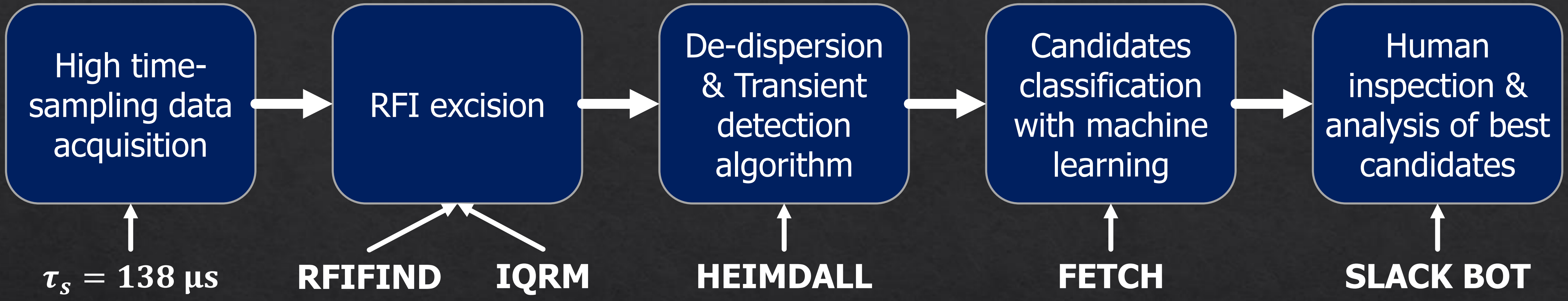

Detection pipeline

Geminardi et al. 2025 (submitted)

High time-sampling data acquisition → RFI excision → De-dispersion & Transient detection algorithm → Candidates classification with machine learning → Human inspection & analysis of best candidates

$\tau_s = 138\ \mu s$ | **RFIFIND**, **IQRM** | **HEIMDALL** | **FETCH** | **SLACK BOT**

Pelliciari, Geminardi et al. ATel 16547 ⟵ **FRB 20240114A** ⟶ **DM = 527 pc cm $^{-3}$**

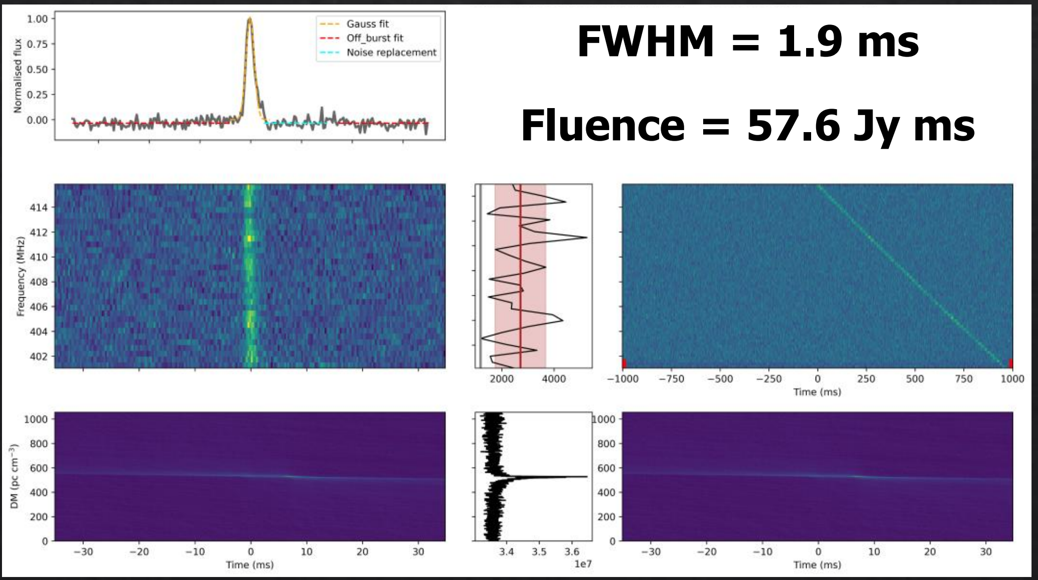

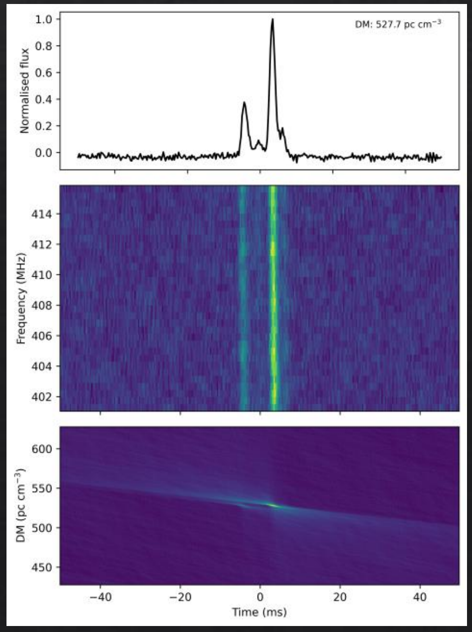

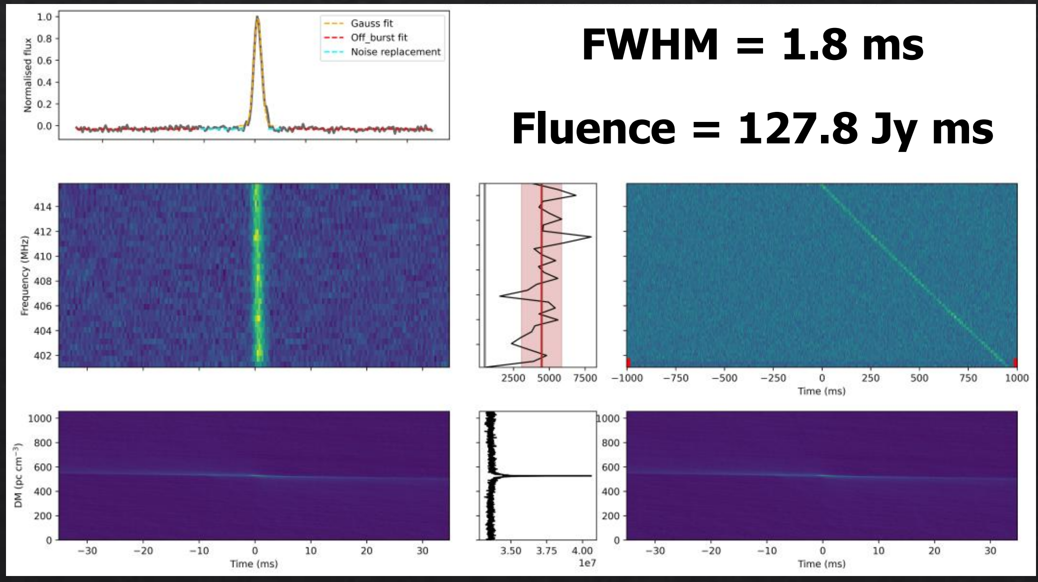

Magnetars

Super-magnetized neutron stars

↓

Magnetic field strength:

$B \sim 10^{14} - 10^{15}$ G

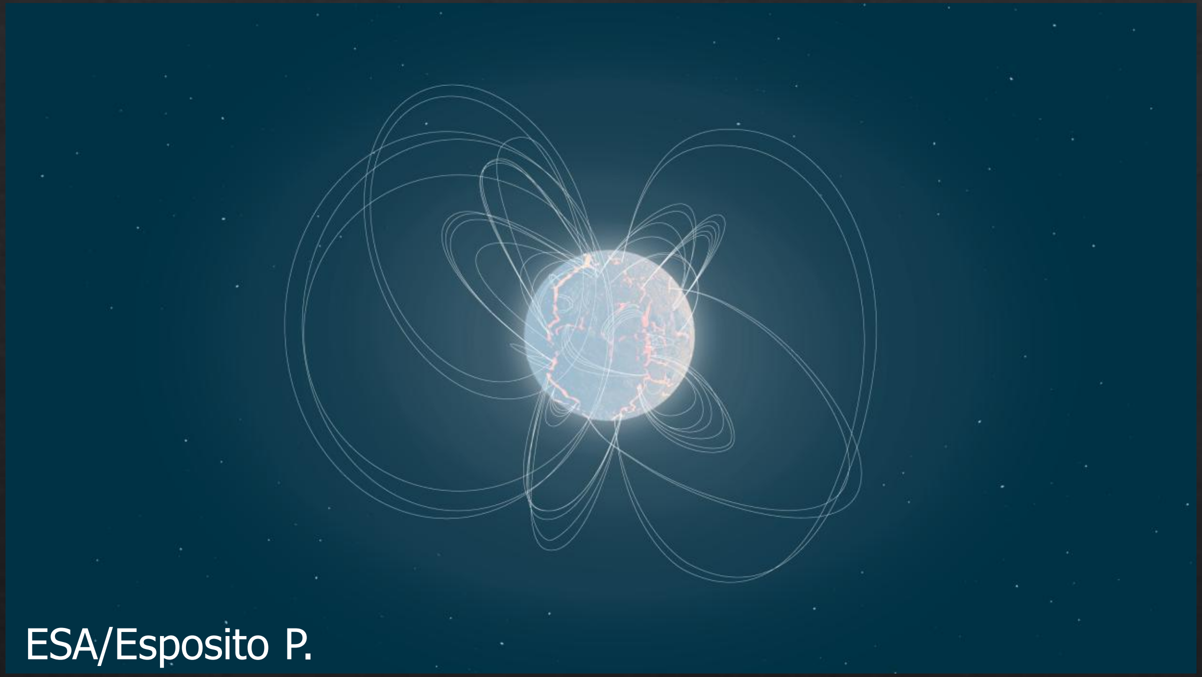

Persistent X-ray sources:

$L_X \sim 10^{34} - 10^{36}$ erg s^{-1}

Transient activity:
Outbursts - Bursts - Giant flares

$L_X \sim 10^{39} - 10^{46}$ erg s^{-1}

Magnetars

Super-magnetized neutron stars

Magnetic field strength:

$B \sim 10^{14} - 10^{15}$ G

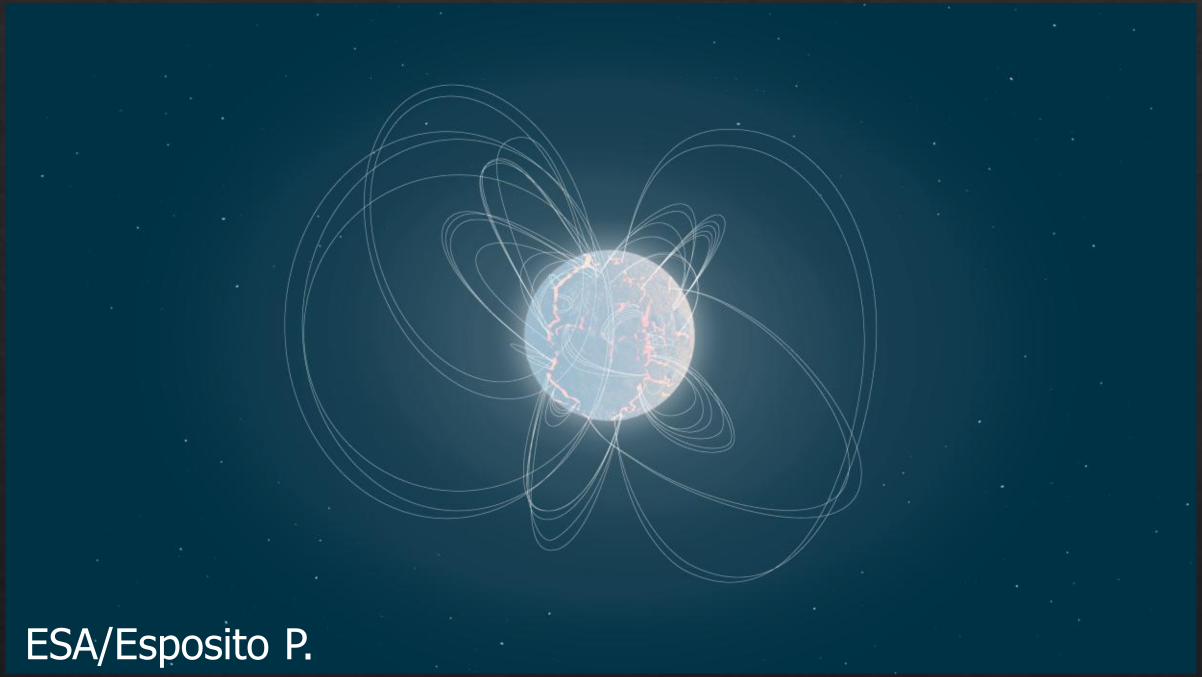

Persistent X-ray sources:

$L_X \sim 10^{34} - 10^{36}$ erg s^{-1}

Transient activity:

Outbursts - Bursts - Giant flares

$L_X \sim 10^{39} - 10^{46}$ erg s^{-1}

Bright radio burst emitting magnetars

SGR J1935+2154 (CHIME/FRB 2020)

$\boxed{E \sim 10^{34} \text{ erg}}$

1E 1547-5408 (Israel et al. 2020)

$E \sim 10^{31}$ erg

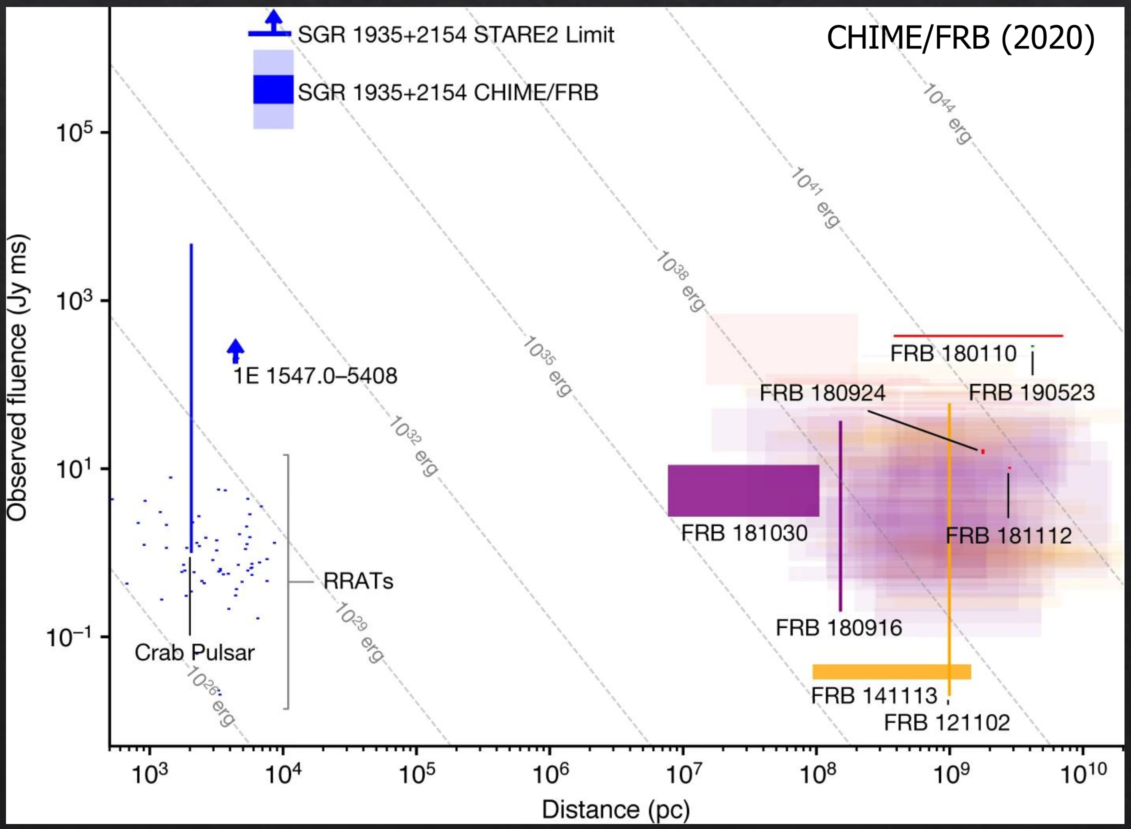

Targets and DMs

Name Geminardi et al. 2025 (submitted)	D (kpc)	n_H (10^{22} cm^{-2})	DM_{NE2001} (pc cm^{-3})	DM_{YMW16} (pc cm^{-3})	DM_{nH} (pc cm^{-3})	DM_{radio} (pc cm^{-3})
3XMM J185246.6+003317	7.1 ± 2.1	1.32 ± 0.05	441^{+275}_{-274}	1020^{+590}_{-633}	440 ± 16	No
SGR 1900+14	12.5 ± 1.7	2.12 ± 0.08	609^{+55}_{-80}	526^{+70}_{-105}	707 ± 26	No
SGR J1935+2154	9.0 ± 2.5	1.6 ± 0.2	293^{+100}_{-114}	320^{+90}_{-119}	533 ± 67	**332.7206(9)**
SGR 2013+34	8.8 ± 2.4	–	279^{+77}_{-110}	302^{+70}_{-133}	–	No
1E 2259+586	3.2 ± 0.2	1.21 ± 0.04	99^{+11}_{-11}	154^{+13}_{-18}	403 ± 13	No
4U 0142+61	3.6 ± 0.4	1.00 ± 0.01	96^{+10}_{-11}	161^{+5}_{-6}	333 ± 3	No
SGR 0418+5729	2.0 ± 0.6	0.115 ± 0.006	63^{+26}_{-25}	93^{+32}_{-55}	38 ± 2	No
SGR 0501+4516	2.0 ± 0.6	0.88 ± 0.01	71^{+27}_{-28}	109^{+27}_{-61}	293 ± 3	No

Targets and DMs

Giant-flare magnetar

FRB-like magnetar

Magnetar candidate

Name Geminardi et al. 2025 (submitted)	D (kpc)	n_H (10^{22} cm^{-2})	DM_{NE2001} (pc cm^{-3})	DM_{YMW16} (pc cm^{-3})	DM_{nH} (pc cm^{-3})	DM_{radio} (pc cm^{-3})
3XMM J185246.6+003317	7.1 ± 2.1	1.32 ± 0.05	441^{+275}_{-274}	1020^{+590}_{-633}	440 ± 16	No
SGR 1900+14	12.5 ± 1.7	2.12 ± 0.08	609^{+55}_{-80}	526^{+70}_{-105}	707 ± 26	No
SGR J1935+2154	9.0 ± 2.5	1.6 ± 0.2	293^{+100}_{-114}	320^{+90}_{-119}	533 ± 67	332.7206(9)
SGR 2013+34	8.8 ± 2.4	–	279^{+77}_{-110}	302^{+70}_{-133}	–	No
1E 2259+586	3.2 ± 0.2	1.21 ± 0.04	99^{+11}_{-11}	154^{+13}_{-18}	403 ± 13	No
4U 0142+61	3.6 ± 0.4	1.00 ± 0.01	96^{+10}_{-11}	161^{+5}_{-6}	333 ± 3	No
SGR 0418+5729	2.0 ± 0.6	0.115 ± 0.006	63^{+26}_{-25}	93^{+32}_{-55}	38 ± 2	No
SGR 0501+4516	2.0 ± 0.6	0.88 ± 0.01	71^{+27}_{-28}	109^{+27}_{-61}	293 ± 3	No

Targets and DMs

Giant-flare magnetar (SGR 1900+14)

FRB-like magnetar (SGR J1935+2154)

Magnetar candidate (SGR 2013+34)

Electron density distribution in the Milky Way

Best-fit relation between DM and n_H

Name Geminardi et al. 2025 (submitted)	D (kpc)	n_H (10^{22} cm^{-2})	DM_{NE2001} (pc cm^{-3})	DM_{YMW16} (pc cm^{-3})	DM_{nH} (pc cm^{-3})	DM_{radio} (pc cm^{-3})
3XMM J185246.6+003317	7.1 ± 2.1	1.32 ± 0.05	441^{+275}_{-274}	1020^{+590}_{-633}	440 ± 16	No
SGR 1900+14	12.5 ± 1.7	2.12 ± 0.08	609^{+55}_{-80}	526^{+70}_{-105}	707 ± 26	No
SGR J1935+2154	9.0 ± 2.5	1.6 ± 0.2	293^{+100}_{-114}	320^{+90}_{-119}	533 ± 67	**332.7206(9)**
SGR 2013+34	8.8 ± 2.4	–	279^{+77}_{-110}	302^{+70}_{-133}	–	No
1E 2259+586	3.2 ± 0.2	1.21 ± 0.04	99^{+11}_{-11}	154^{+13}_{-18}	403 ± 13	No
4U 0142+61	3.6 ± 0.4	1.00 ± 0.01	96^{+10}_{-11}	161^{+5}_{-6}	333 ± 3	No
SGR 0418+5729	2.0 ± 0.6	0.115 ± 0.006	63^{+26}_{-25}	93^{+32}_{-55}	38 ± 2	No
SGR 0501+4516	2.0 ± 0.6	0.88 ± 0.01	71^{+27}_{-28}	109^{+27}_{-61}	293 ± 3	No

Cordes & Lazio 2002 | Yao et al. 2017 | He et al. 2013

Targets and DMs

Name	D (kpc)	n_H (10^{22} cm^{-2})	DM_{NE2001} (pc cm^{-3})	DM_{YMW16} (pc cm^{-3})	DM_{nH} (pc cm^{-3})	DM_{radio} (pc cm^{-3})
3XMM J185246.6+003317	7.1 ± 2.1	1.32 ± 0.05	441^{+275}_{-274}	1020^{+590}_{-633}	440 ± 16	No
SGR 1900+14	12.5 ± 1.7	2.12 ± 0.08	609^{+55}_{-80}	526^{+70}_{-105}	707 ± 26	No
SGR J1935+2154	9.0 ± 2.5	1.6 ± 0.2	293^{+100}_{-114}	320^{+90}_{-119}	533 ± 67	332.7206(9)
SGR 2013+34	8.8 ± 2.4	–	279^{+77}_{-110}	302^{+70}_{-133}	–	No
1E 2259+586	3.2 ± 0.2	1.21 ± 0.04	99^{+11}_{-11}	154^{+13}_{-18}	403 ± 13	No
4U 0142+61	3.6 ± 0.4	1.00 ± 0.01	96^{+10}_{-11}	161^{+5}_{-6}	333 ± 3	No
SGR 0418+5729	2.0 ± 0.6	0.115 ± 0.006	63^{+26}_{-25}	93^{+32}_{-55}	38 ± 2	No
SGR 0501+4516	2.0 ± 0.6	0.88 ± 0.01	71^{+27}_{-28}	109^{+27}_{-61}	293 ± 3	No

Geminardi et al. 2025 (submitted)

Giant-flare magnetar

FRB-like magnetar

Magnetar candidate

Electron density distribution in the Milky Way

Best-fit relation between DM and n_H

Cordes & Lazio 2002

Yao et al. 2017

He et al. 2013

+ 5 ephemeral pulsating magnetars during outburst phases

Monitoring & Candidates

Daily cadence observations ($\sim$ 560 hours observed)

↓

DM range
20 – 3000 pc cm $^{-3}$

Width range
0.1 – 70 ms

↓

$\sim$ 1.3 million candidates found

↓

$\sim$ 20000 candidates selected by FETCH

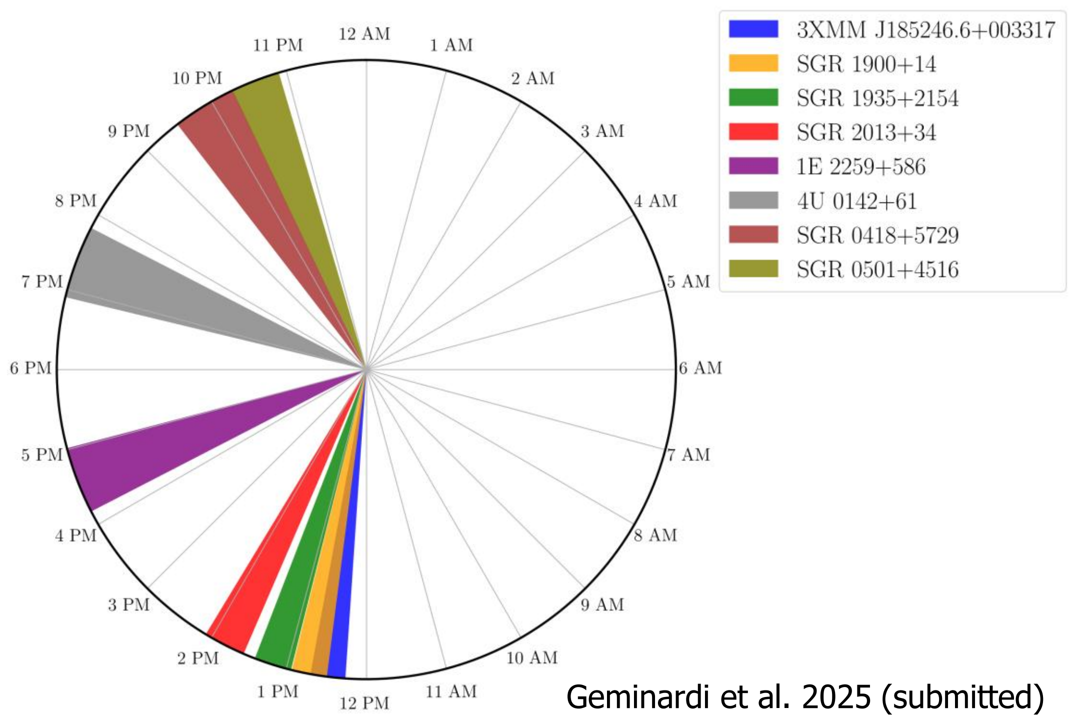

Geminardi et al. 2025 (submitted)

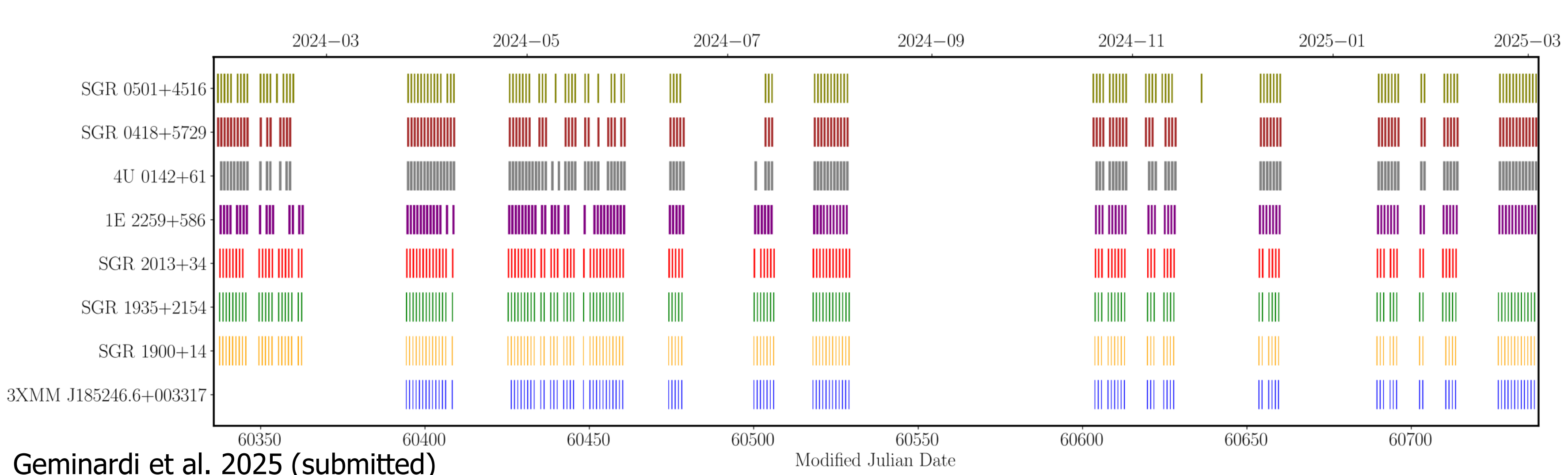

Geminardi et al. 2025 (submitted)

Monitoring & Candidates

Daily cadence observations (~ 560 hours observed)

↓

DM range $20 - 3000$ **pc cm** $^{-3}$

Width range **0.1 – 70 ms**

↓

~ 1.3 million candidates found

↓

~ 20000 candidates selected by FETCH

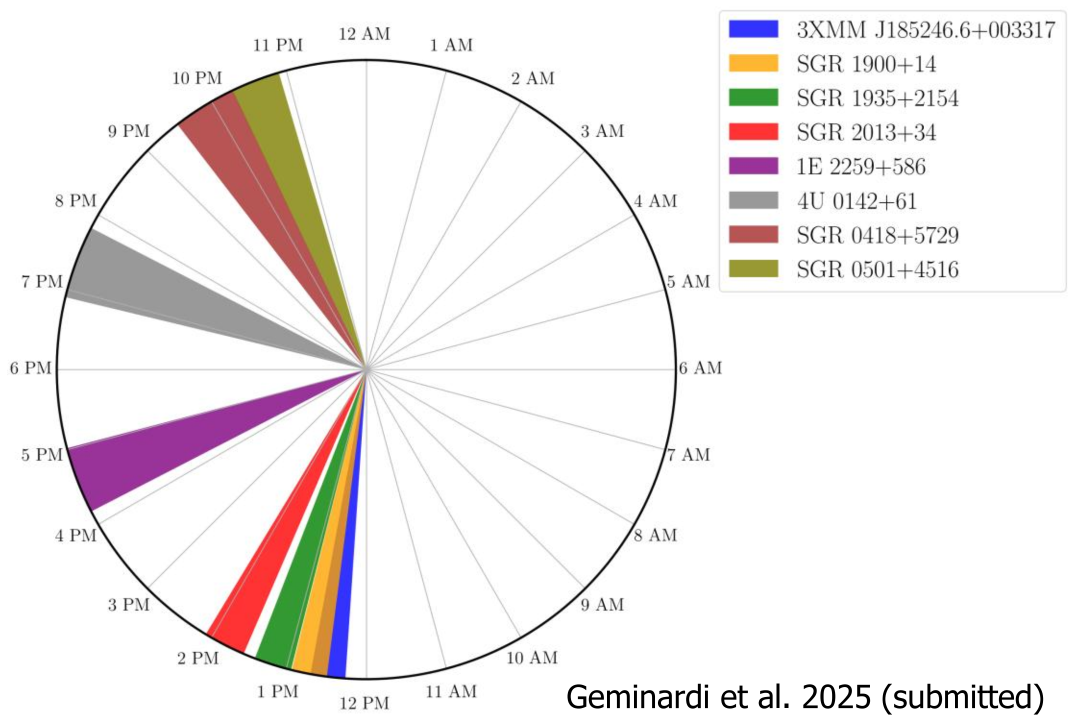

Geminardi et al. 2025 (submitted)

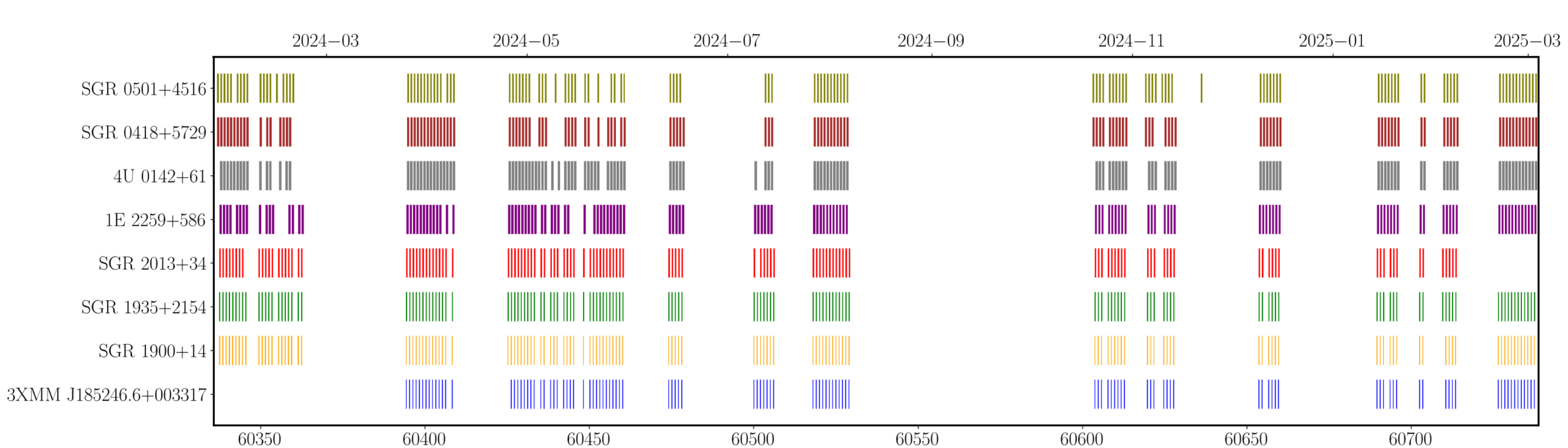

Geminardi et al. 2025 (submitted)

No radio bursts associated to the magnetars

Campaign sensitivity

$$F_\nu = {}^{S}/_{N} \, \frac{\mathrm{SEFD}}{A\sqrt{N_p N_c (1-\xi)\Delta\nu_{ch} w}} \frac{1}{G(\mathrm{ToA})}$$

1 ms burst $\downarrow$ **S/N = 7**

$$E_{min} = (1.34 - 2.72) \times 10^{20} \left(\frac{D}{[\mathrm{pc}]}\right) \text{ erg}$$

Name Geminardi et al. 2025 (submitted)	Total exposure (hours)	E_{min} 10^{26} (erg)
3XMM J185246.6+003317	33.46	67 – 137
SGR 1900+14	40.58	209 – 424
SGR J1935+2154	52.34	108 – 220
SGR 2013+34	63.38	104 – 210
1E 2259+586	97.03	14 – 28
4U 0142+61	116.08	17 – 35
SGR 0418+5729	92.95	5 – 11
SGR 0501+4516	70.10	5 – 11
All magnetars	565.92	5 – 424
All magnetars (NO SGR 2013+34)	502.54	5 – 424

Campaign sensitivity

$$F_\nu = S/N \frac{SEFD}{A\sqrt{N_p N_c (1-\xi)\Delta\nu_{ch} w}} \frac{1}{G(ToA)}$$

1 ms burst **S/N = 7**

$$E_{min} = (1.34 - 2.72) \times 10^{20} \left(\frac{D}{[pc]}\right) \textbf{ erg}$$

Name Geminardi et al. 2025 (submitted)	Total exposure (hours)	E_{min} 10^{26} (erg)
3XMM J185246.6+003317	33.46	67 – 137
SGR 1900+14	40.58	209 – 424
SGR J1935+2154	52.34	108 – 220
SGR 2013+34	63.38	104 – 210
1E 2259+586	97.03	14 – 28
4U 0142+61	116.08	17 – 35
SGR 0418+5729	92.95	5 – 11
SGR 0501+4516	70.10	5 – 11
All magnetars	565.92	5 – 424
All magnetars (NO SGR 2013+34)	502.54	5 – 424

Detectable events

- **FRB-like radio bursts**
- **Giant pulses-like**
- **Most energetic pulses from RRATs and pulsars**

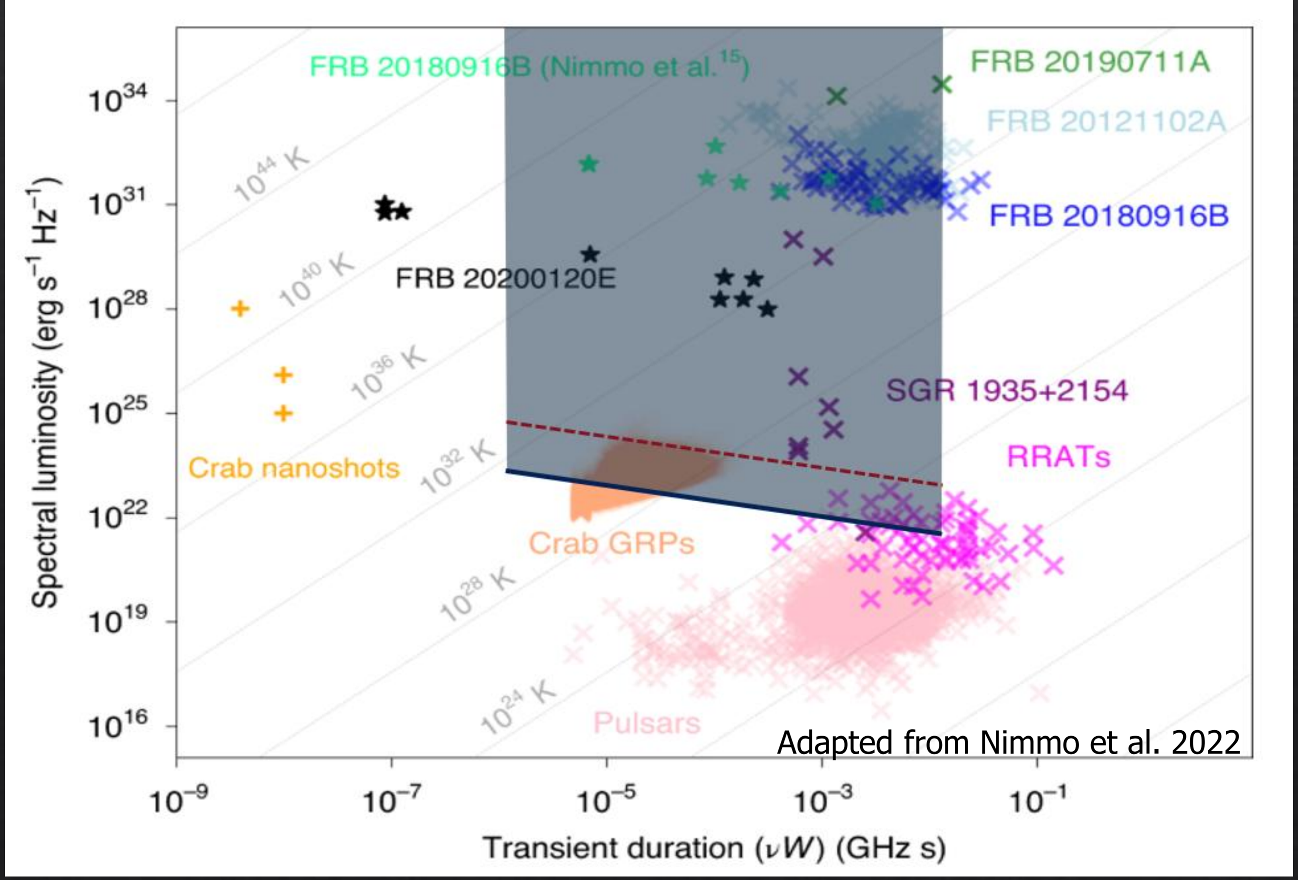

Upper limits

SGR J1935+2154 bursting activity

↓

1 FRB-like event (CHIME + Bochenek 2020) and few fainter events

POISSON DISTRIBUTION

Name	$\mathcal{R}(E > E_{min})$
Geminardi et al. 2025 (submitted)	(yr^{-1})
3XMM J185246.6+003317	< 785
SGR 1900+14	< 647
SGR J1935+2154	< 502
SGR 2013+34	< 414
1E 2259+586	< 271
4U 0142+61	< 226
SGR 0418+5729	< 283
SGR 0501+4516	< 375
All magnetars	< 46
All magnetars (NO SGR 2013+34)	< 52

Upper limits & Power-law distribution

SGR J1935+2154 bursting activity

↓

1 FRB-like event (CHIME + Bochenek 2020) and few fainter events

POISSON DISTRIBUTION

Name	$\mathcal{R}(E > E_{min})$
Geminardi et al. 2025 (submitted)	(yr^{-1})
3XMM J185246.6+003317	< 785
SGR 1900+14	< 647
SGR J1935+2154	< 502
SGR 2013+34	< 414
1E 2259+586	< 271
4U 0142+61	< 226
SGR 0418+5729	< 283
SGR 0501+4516	< 375
All magnetars	< 46
All magnetars (NO SGR 2013+34)	< 52

Rate of detectable events $(E > E_{min})$

$$R(\lambda_{mag}, \gamma; E > E_{min,j}) = \int_{E_{min,j}}^{E_{max}} K_0 \left(\frac{E}{E_0}\right)^{-\gamma} dE$$

↓

2 free parameters

λ_{mag} → **Rate of events with energy greater than the SGR J1935 FRB-like event** $(E > E_0)$

γ → **Slope of the power-law energy distribution of single bursts**

Resulting plots

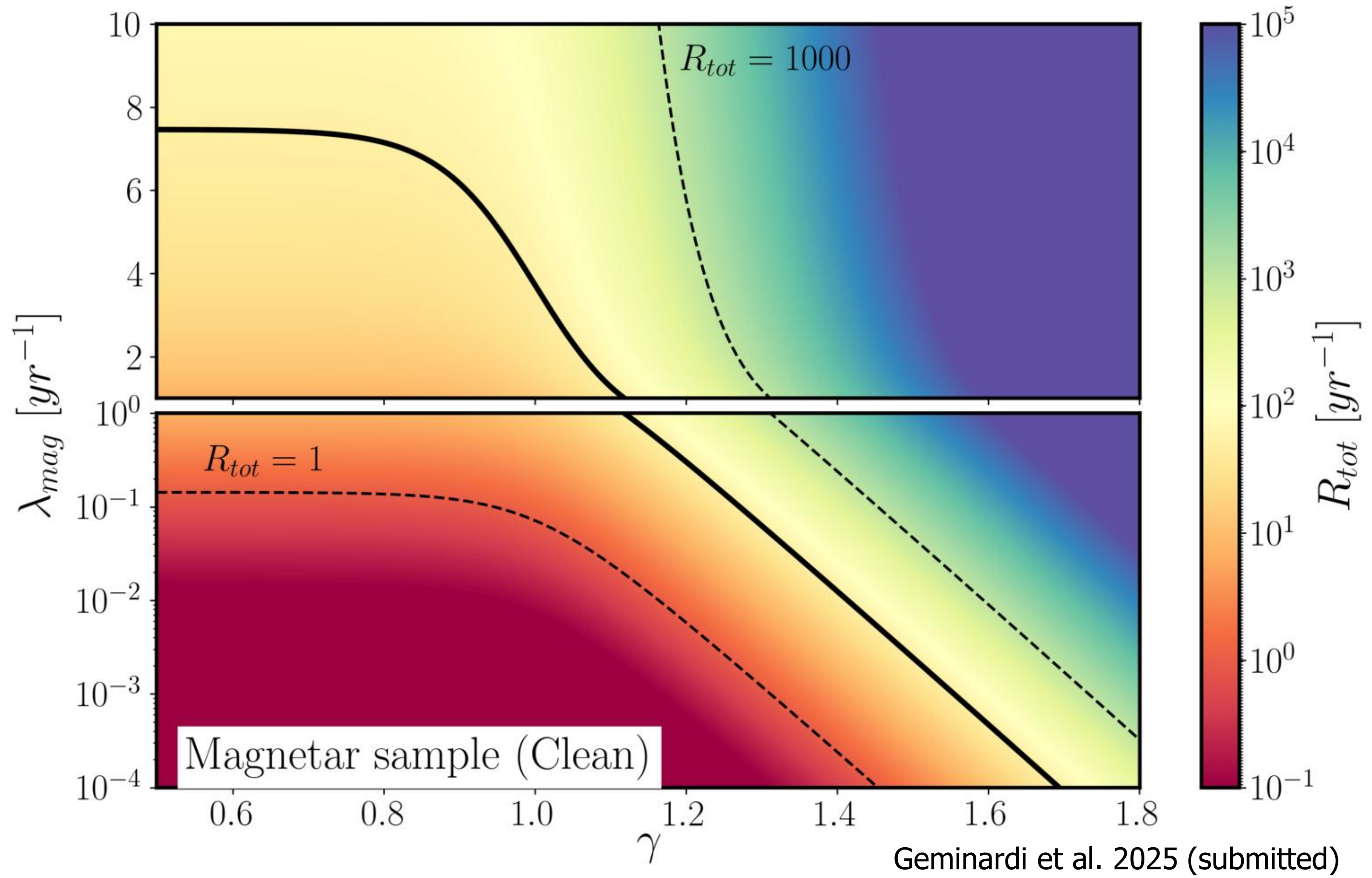

Geminardi et al. 2025 (submitted)

Resulting plots

Steeper slope → Many low-energy detectable events

$\gamma \lesssim 1.1$

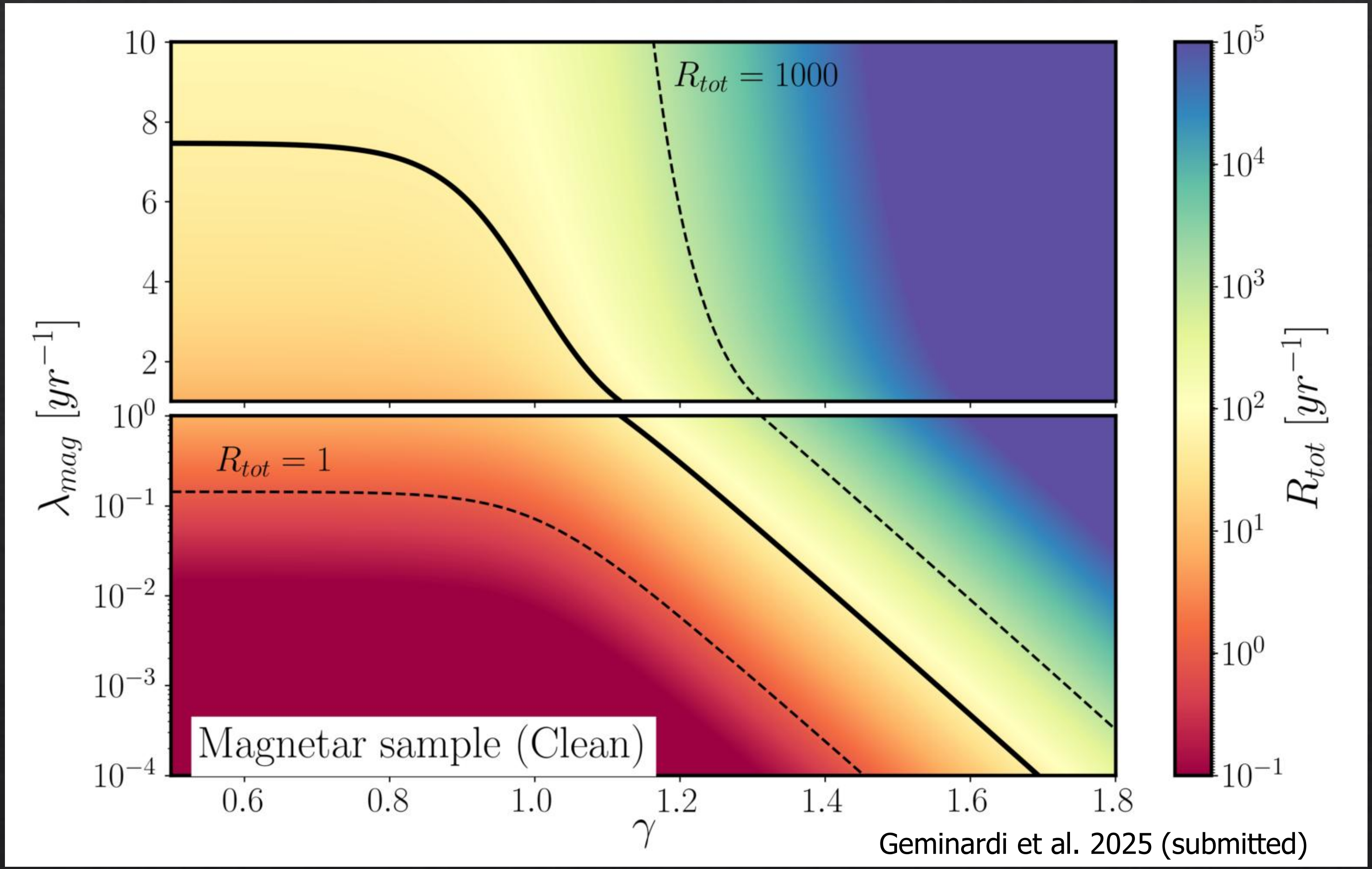

$\gamma \gtrsim 1.4$

Flatter slope → Few low-energy events and strong λ_{mag} dependence

Resulting plots

Upper limit for flat power-law
↓
$\lambda_{mag} < 7.4$ **yr** $^{-1}$

$\gamma \lesssim 1.1$

Flatter slope
↓
Few low-energy events and strong λ_{mag} dependence

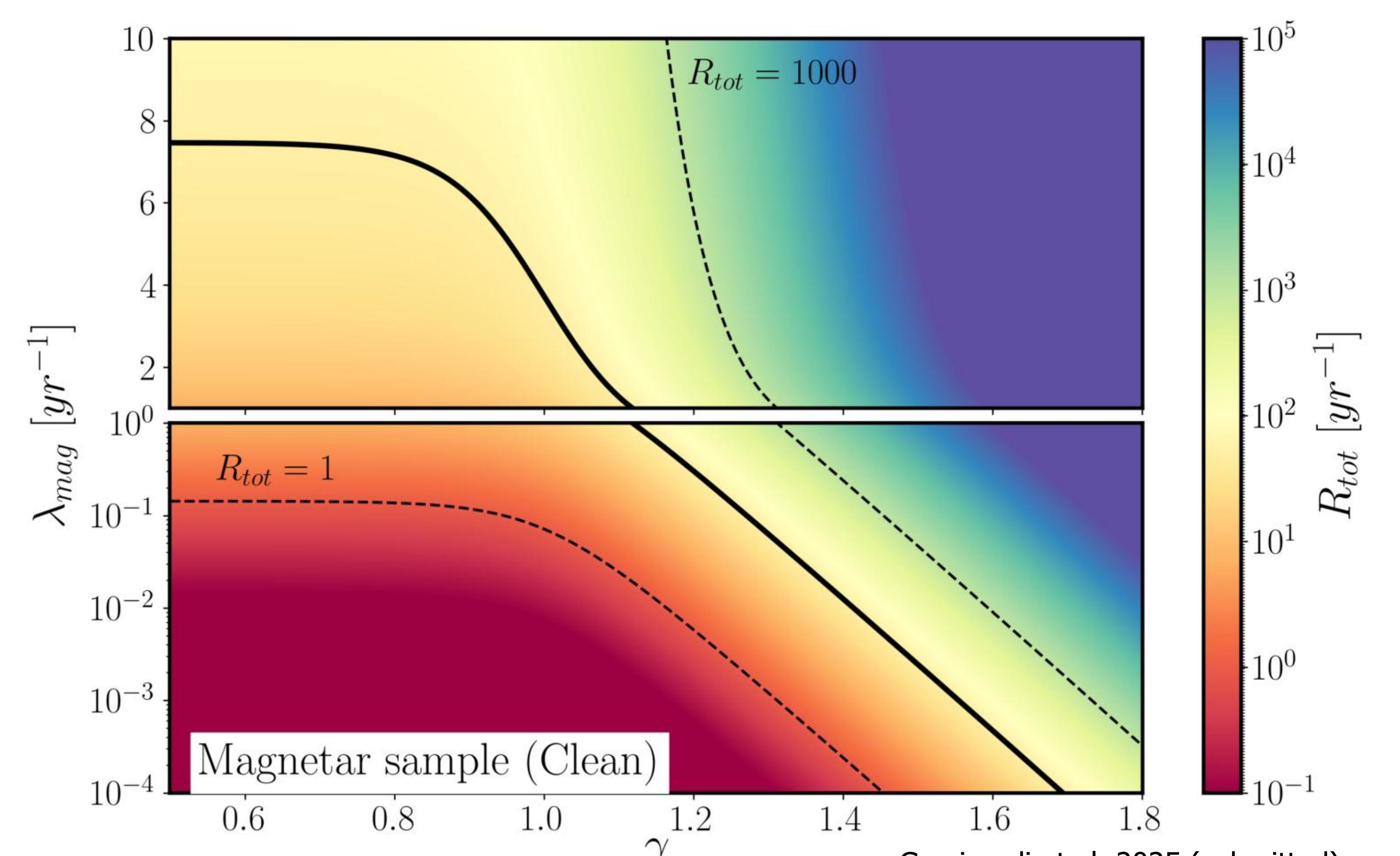

Geminardi et al. 2025 (submitted)

Steeper slope
↓
Many low-energy detectable events

$\gamma \gtrsim 1.4$

Upper limit for steep power-law
↓
$\lambda_{mag} < 10^{-3}$ **yr** $^{-1}$

DISFAVOURED BY THE RADIO BURST DETECTIONS FROM MAGNETARS

Comparison with other FRB works

CHIME/FRB 2020

↓

SGR J1935 + 15 nearby galaxies

↓

$\boxed{0.007 < \lambda_{mag} < 0.4\ \text{yr}^{-1}}$

NC (Pelliciari et al. 2023)

↓

7 nearby galaxies

↓

$\lambda_{mag} < 0.42\ \text{yr}^{-1}$

Comparison with other FRB works

CHIME/FRB 2020

↓

SGR J1935 + 15 nearby galaxies

↓

$\boxed{0.007 < \lambda_{mag} < 0.4 \text{ yr}^{-1}}$

NC (Pelliciari et al. 2023)

↓

7 nearby galaxies

↓

$\lambda_{mag} < 0.42 \text{ yr}^{-1}$

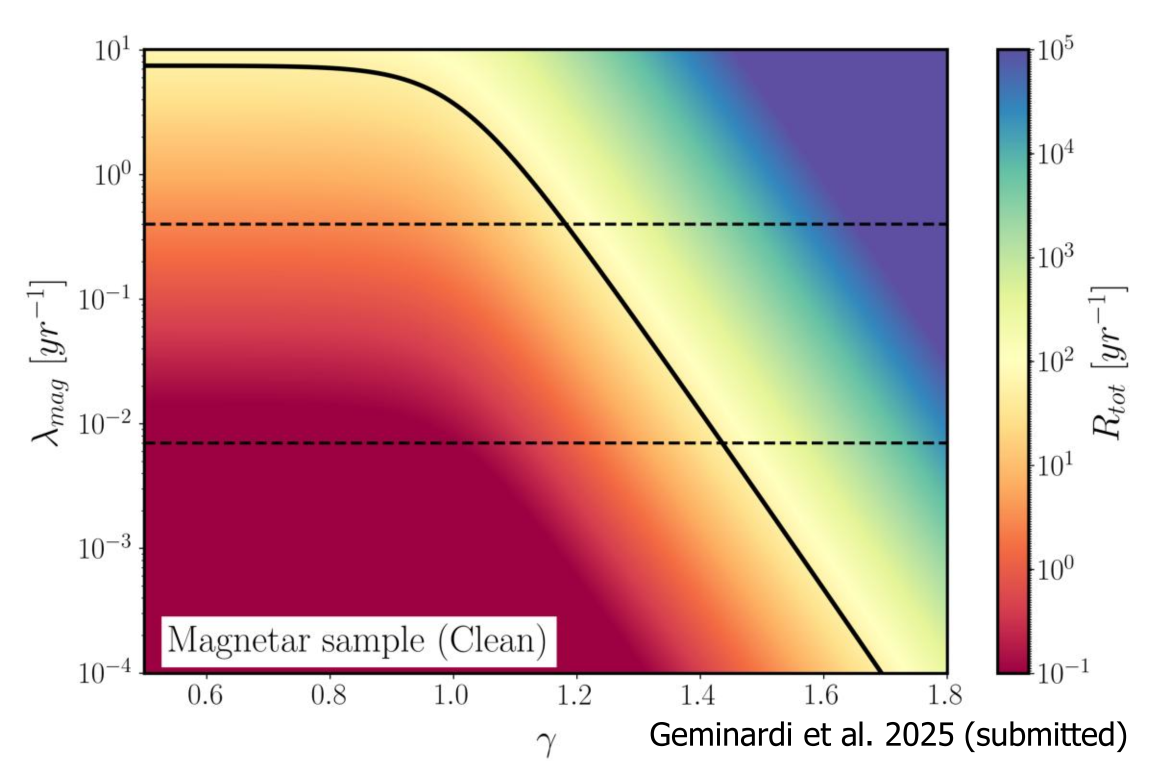

Geminardi et al. 2025 (submitted)

Comparison with other FRB works

CHIME/FRB 2020

SGR J1935 + 15 nearby galaxies

$0.007 < \lambda_{mag} < 0.4$ yr $^{-1}$

NC (Pelliciari et al. 2023)

7 nearby galaxies

$\lambda_{mag} < 0.42$ yr $^{-1}$

NC NEW

7 Galactic magnetars + 7 nearby galaxies

$\lambda_{mag} < 0.043$ yr $^{-1}$

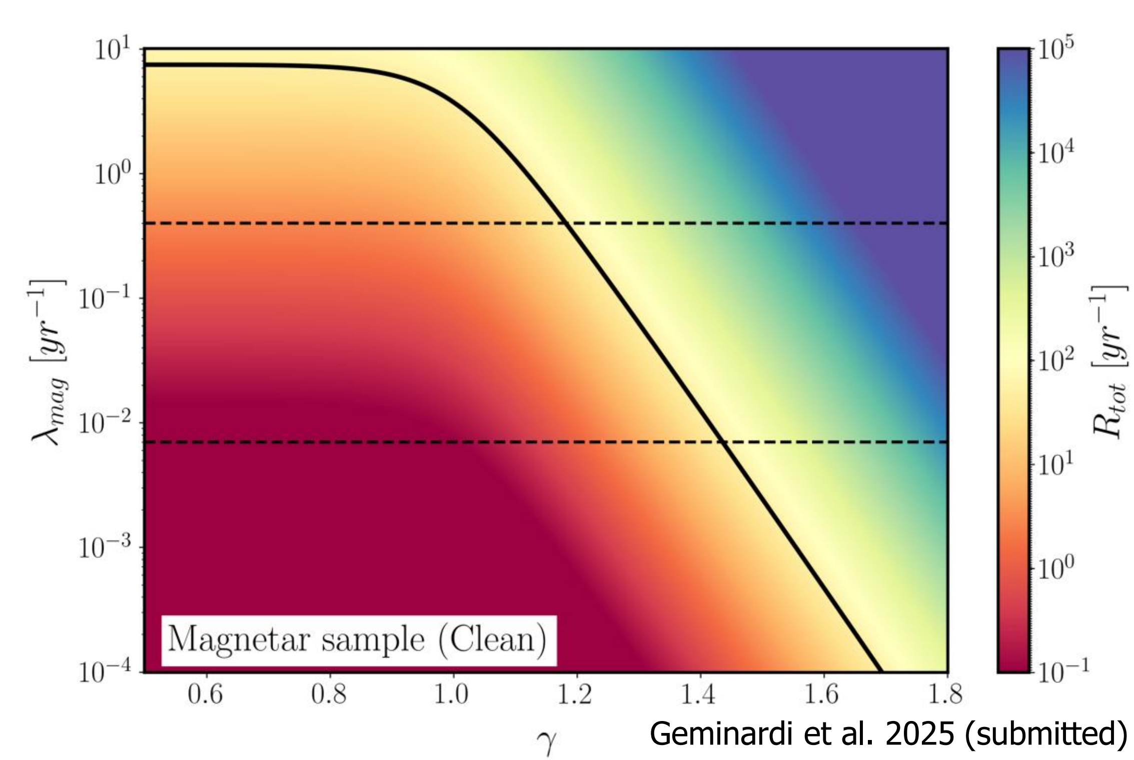

Geminardi et al. 2025 (submitted)

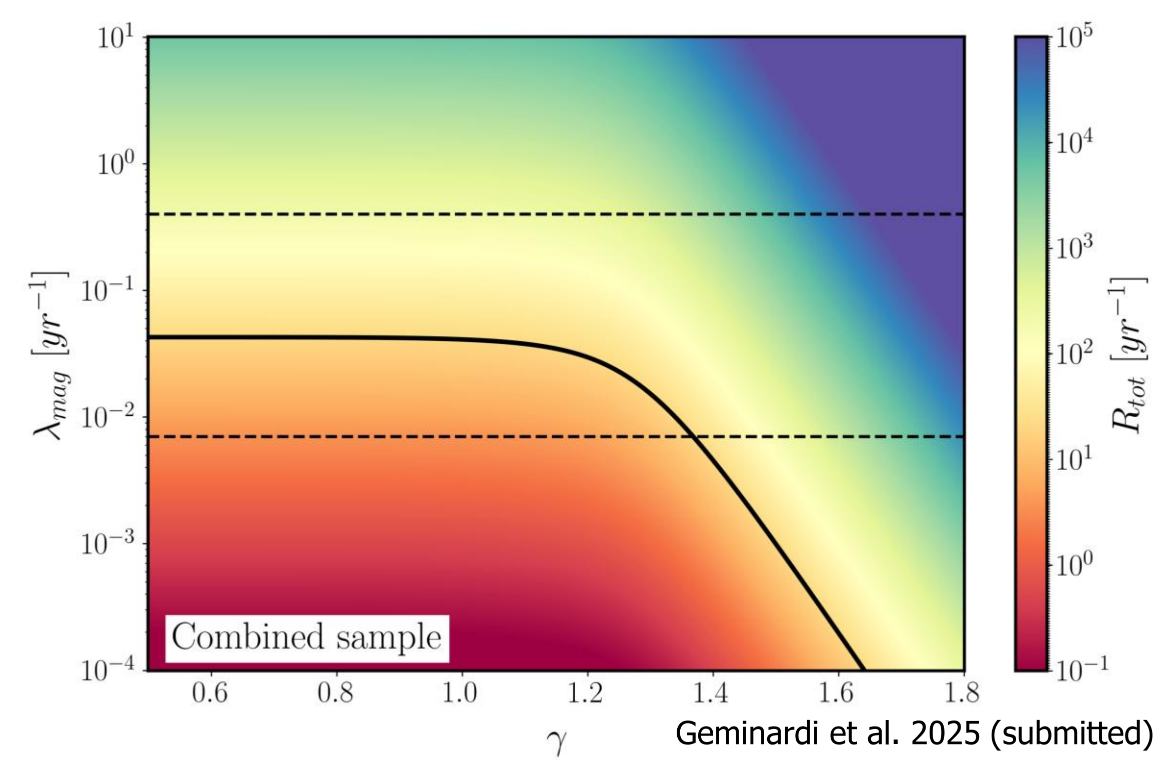

Geminardi et al. 2025 (submitted)

Summary & Conclusions

- **We observed 7 Galactic magnetars + 1 candidate for $\sim$ 560 hours.**
- **We are sensitive to FRB-like events, giant pulses and pulsar-like emission.**
- **No detections → $\mathrm{R_{tot}} < 52$ yr $^{-1}$.**
- **We constrained the energy distribution using our limits and the literature ones.**

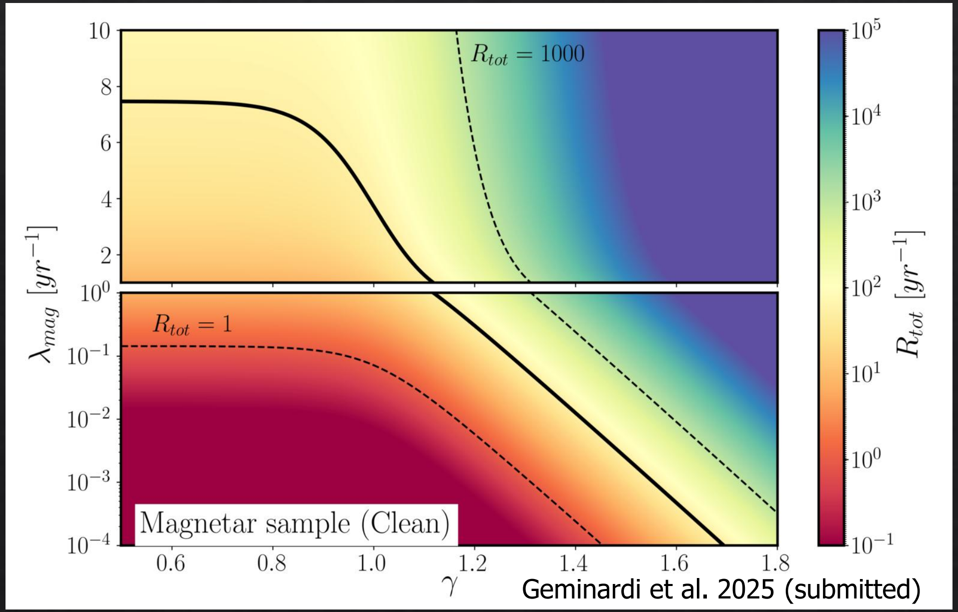

Geminardi et al. 2025 (submitted)

- **Our Galactic observations are sensitive to the low-energy events, constraining the energy distribution.**
- **Power-laws steeper than $\gamma \simeq 1.4$ are disfavoured by the current limits.**
- **Our results are in tension with the models that attempt to use magnetar emission to explain the FRB all-sky rate.**

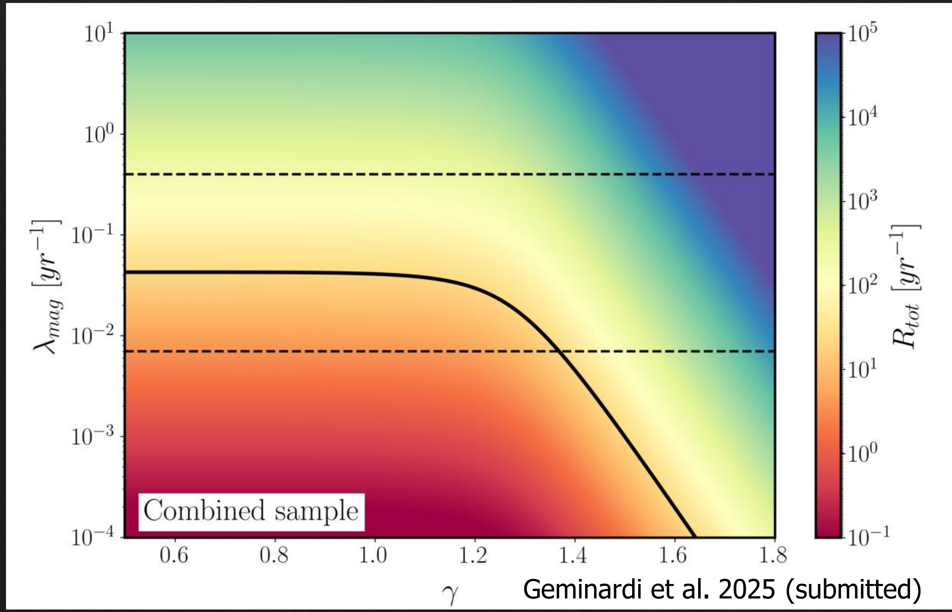

Geminardi et al. 2025 (submitted)

THANK YOU FOR THE ATTENTION!

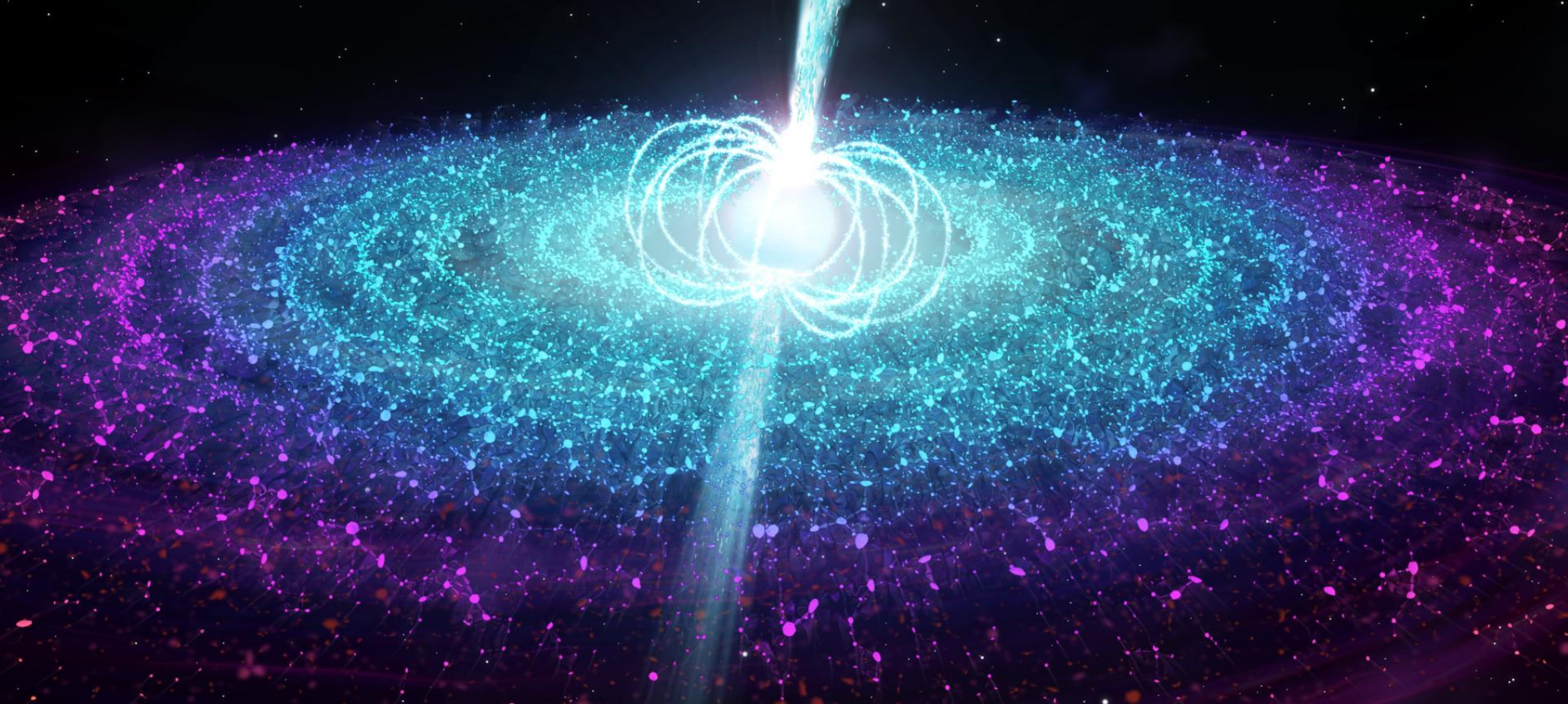

Table 1. Localization and predicted Galactic DM contributions for the magnetar sample.

Name	Gal L (deg)	Gal B (deg)	D (kpc)	n_H (10^{22} cm^{-2})	DM_{NE2001} (pc cm^{-3})	DM_{YMW16} (pc cm^{-3})	DM_{nH} (pc cm^{-3})	DM_{radio} (pc cm^{-3})	Ref.
3XMM J185246.6+003317	33.5785548	-0.0450683	7.1 ± 2.1	1.32 ± 0.05	441^{+275}_{-274}	1020^{+590}_{-633}	440 ± 16	No	1
SGR 1900+14	43.0034808	0.8520327	12.5 ± 1.7	2.12 ± 0.08	609^{+55}_{-80}	526^{+70}_{-105}	707 ± 26	No	2,3
SGR J1935+2154	57.2467449	0.8189765	9.0 ± 2.5	1.6 ± 0.2	293^{+100}_{-114}	320^{+90}_{-119}	533 ± 67	Yes ($\sim$ 332.7)	4,5,6
SGR 2013+34	72.3203222	-0.1010242	8.8 ± 2.4	–	279^{+77}_{-110}	302^{+70}_{-133}	–	No	7
1E 2259+586	109.0873535	-0.9957528	3.2 ± 0.2	1.21 ± 0.04	99^{+11}_{-11}	154^{+13}_{-18}	403 ± 13	No	8,9
4U 0142+61	129.3839879	-0.4307465	3.6 ± 0.4	1.00 ± 0.01	96^{+10}_{-11}	161^{+5}_{-6}	333 ± 3	No	10,11
SGR 0418+5729	147.9790422	5.1191370	2.0 ± 0.6	0.115 ± 0.006	63^{+26}_{-25}	93^{+32}_{-55}	38 ± 2	No	12,13
SGR 0501+4516	161.5466873	1.9489249	2.0 ± 0.6	0.88 ± 0.01	71^{+27}_{-28}	109^{+27}_{-61}	293 ± 3	No	14,15

Notes. The second and third columns list the Galactic latitude and longitude of the targets, respectively. The fourth column contains the distances adopted for the magnetars; the distances of 3XMM J185246.6+003317, SGR 2013+34, SGR 0418+5729 and SGR 0501+4516 are strongly discussed in the literature, therefore we choose conservative uncertainty intervals of ±30% around the most credible values. The fifth column represents the hydrogen column density derived from high-energy observations. The sixth and seventh columns show the inferred DM contributions, assuming our values for the distances, using the electron density distribution models Cordes & Lazio (2002) and Yao et al. (2017), respectively. The eighth column contains the DM contribution obtained with the best-fit relation between n_H and DM in He et al. (2013). Finally, the last column shows the DM obtained with radio observations; this value is available only for SGR J1935+2154, as the other magnetars of our sample have never been detected at radio wavelengths.

References. [1] Rea et al. (2014); [2] Mereghetti et al. (2006); [3] Davies et al. (2009); [4] Zhong et al. (2020); [5] Israel et al. (2016); CHIME/FRB Collaboration et al. (2020); [7] Sakamoto et al. (2011a); [8] Kothes & Foster (2012); [9] Pizzocaro et al. (2019); [10] Durant & van Kerkwijk (2006); [11] Rea et al. (2007); [12] van der Horst et al. (2010); [13] Rea et al. (2013b); [14] Lin et al. (2011); [15] Camero et al. (2014).

Table 2. Inferred upper limits on the magnetars sample.

Name	Total exposure (hours)	E_{min} 10^{26} (erg)	$\mathcal{R}(E > E_{min})$ (yr^{-1})	$\mathcal{R}(E > E_{J1935})$, $\gamma = 1$ (yr^{-1})	$\mathcal{R}(E > E_{J1935})$, $\gamma = 1.3$ (yr^{-1})	$\mathcal{R}(E > E_{J1935})$, $\gamma = 1.6$ (yr^{-1})
3XMM J185246.6+003317	33.46	67 – 137	< 785	< 400	< 8.78	< 0.10
SGR 1900+14	40.58	209 – 424	< 647	< 342	< 10.19	< 0.17
SGR J1935+2154	52.34	108 – 220	< 502	< 260	< 6.48	< 0.09
SGR 2013+34	63.38	104 – 210	< 414	< 214	< 5.36	< 0.07
1E 2259+586	97.03	14 – 28	< 271	< 131	< 1.91	< 0.01
4U 0142+61	116.08	17 – 35	< 226	< 110	< 1.71	< 0.01
SGR 0418+5729	92.95	5 – 11	< 283	< 133	< 1.49	< 0.01
SGR 0501+4516	70.10	5 – 11	< 375	< 176	< 1.97	< 0.01
All magnetars	565.92	5 – 424	< 46	< 2.92	< 0.05	$< 4.04 \times 10^{-4}$
All magnetars (NO SGR 2013+34)	502.54	5 – 424	< 52	< 3.74	< 0.06	$< 4.76 \times 10^{-4}$

Notes. The second column contains the amount of hours observed on each target. The third column represents the interval of the minimum detectable energy above which we defined the upper limit on the rate of events. The fourth column shows the Poissonian upper limit at 95% confidence level on the observable burst rate. The last three columns list the inferred upper limits on the rates of events with an energy grater than the FRB-like event of the magnetar SGR J1935+2154 using Eq. 7 for 3 different power-law indexes (as indicated in each column).

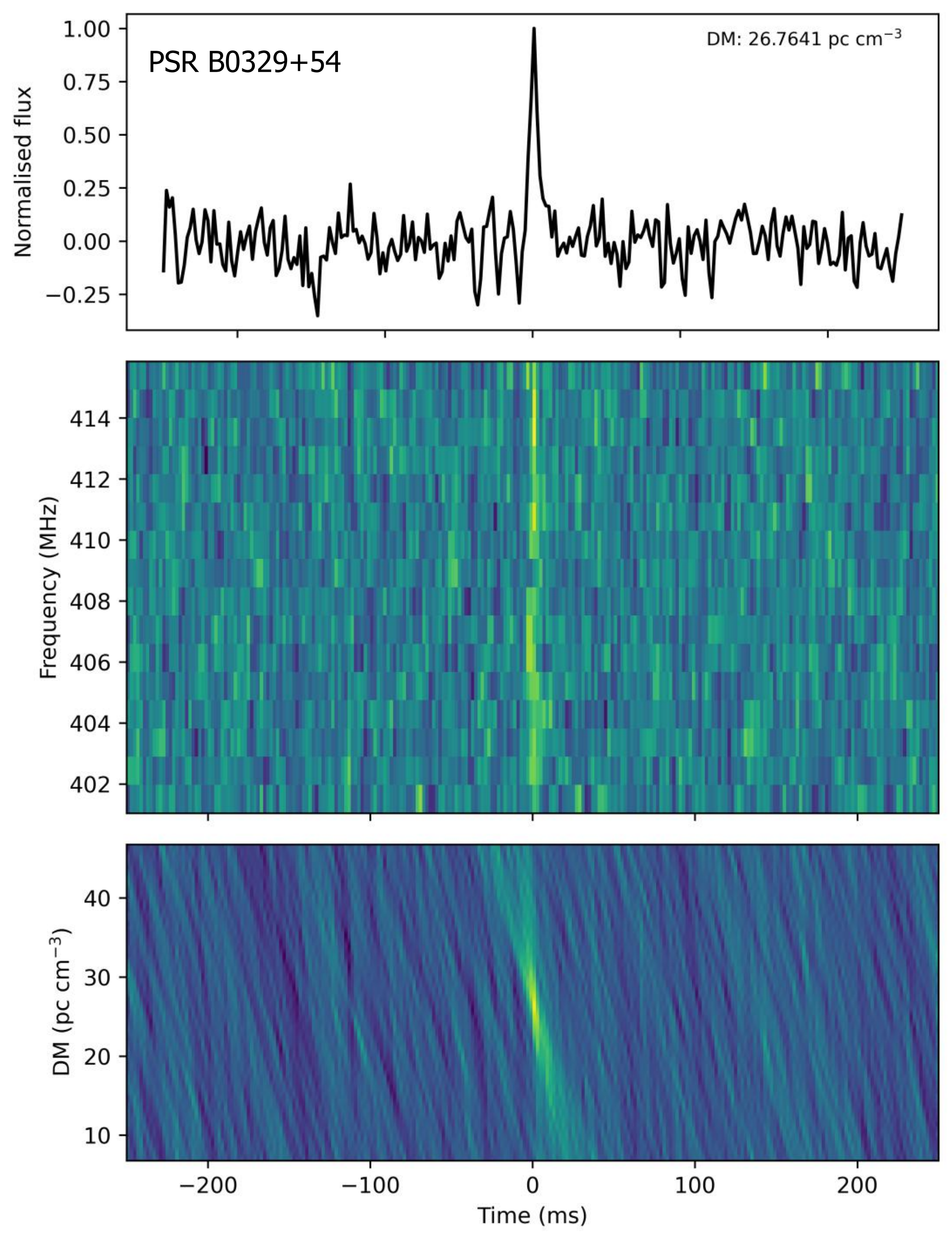
PSR B0329+54
DM: 26.7641 pc cm^{-3}
Normalised flux
1.00
0.75
0.50
0.25
0.00
−0.25
Frequency (MHz)
414
412
410
408
406
404
402
DM (pc cm^{-3})
40
30
20
10
−200
−100
0
100
200
Time (ms)

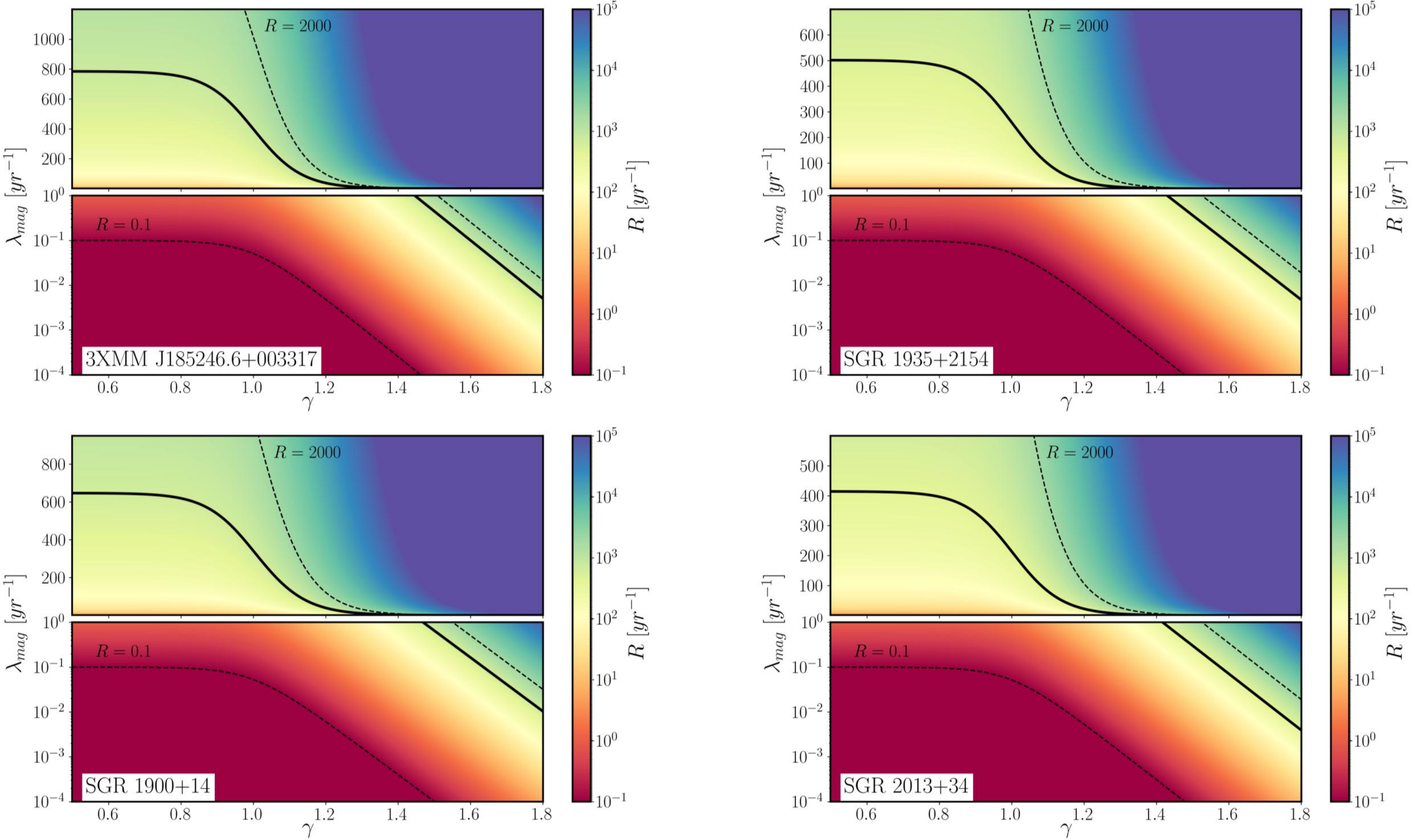

R = 2000
R = 0.1
3XMM J185246.6+003317
SGR 1935+2154
SGR 1900+14
SGR 2013+34
λ_{mag} $[yr^{-1}]$
R $[yr^{-1}]$
γ

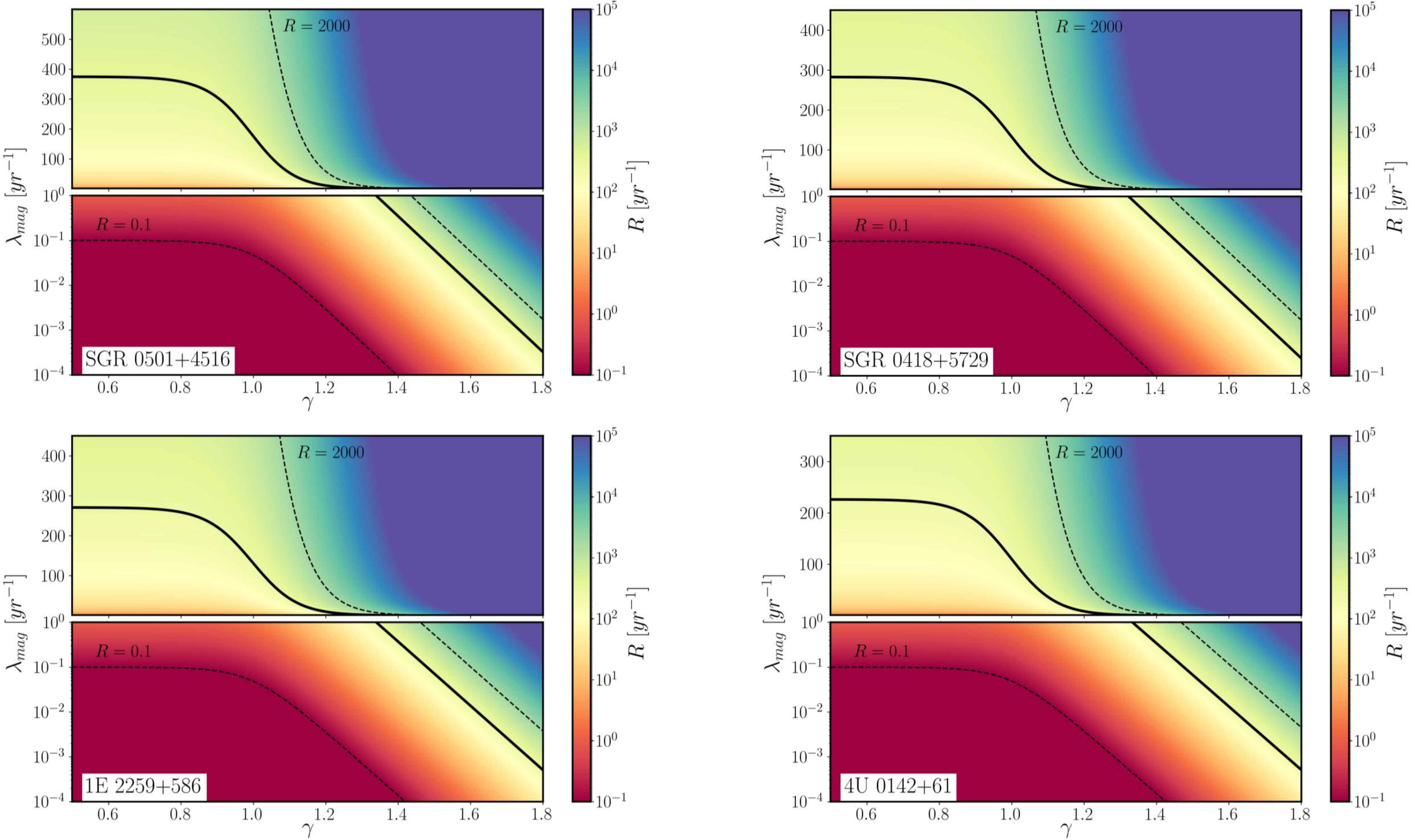

SGR 0501+4516
SGR 0418+5729
1E 2259+586
4U 0142+61
$R = 2000$
$R = 0.1$
$\lambda_{mag}\ [yr^{-1}]$
$R\ [yr^{-1}]$
γ

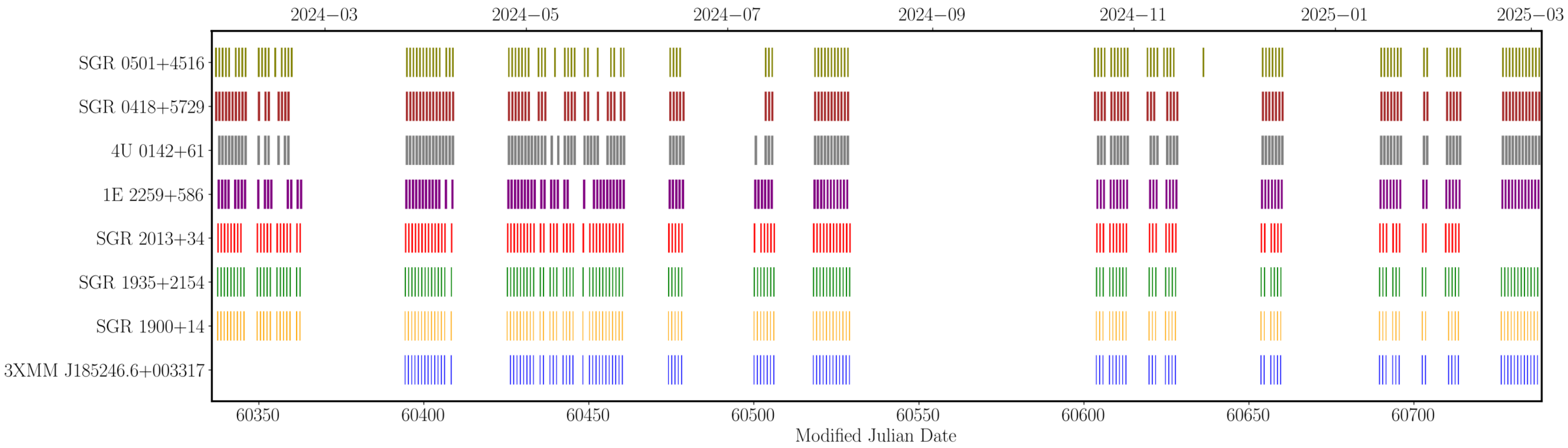
2024−03
2024−05
2024−07
2024−09
2024−11
2025−01
2025−03
SGR 0501+4516
SGR 0418+5729
4U 0142+61
1E 2259+586
SGR 2013+34
SGR 1935+2154
SGR 1900+14
3XMM J185246.6+003317
60350
60400
60450
60500
60550
60600
60650
60700
Modified Julian Date

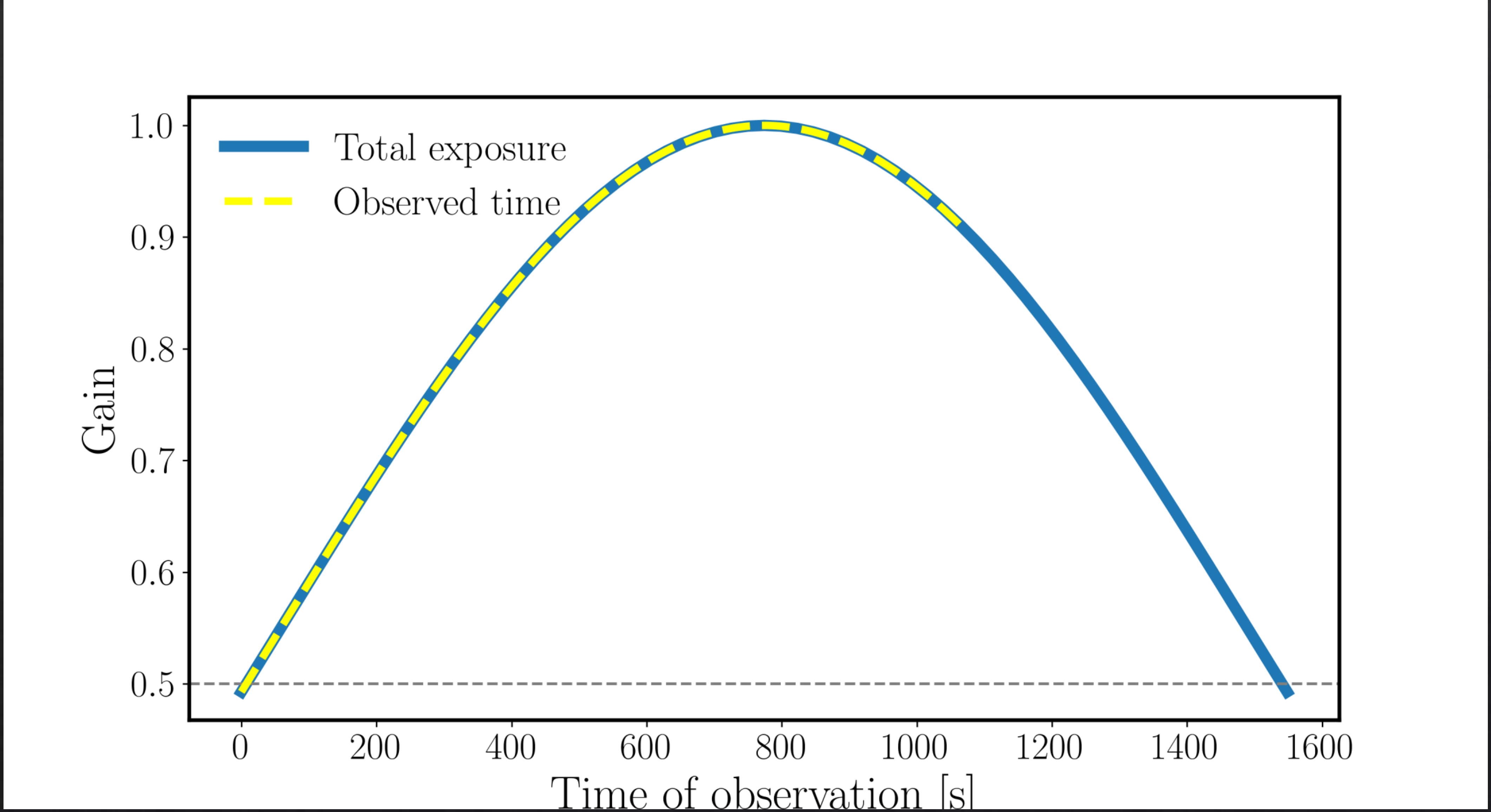

Total exposure
Observed time
Gain
1.0
0.9
0.8
0.7
0.6
0.5
0
200
400
600
800
1000
1200
1400
1600
Time of observation [s]

FRB observations & Detections

NC long-term monitoring

FRB 20240114A

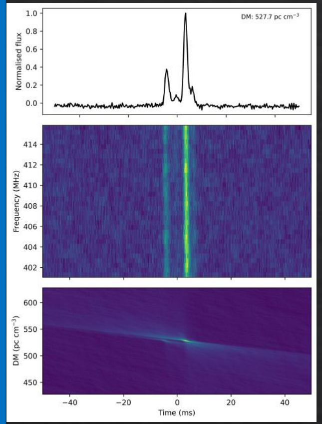

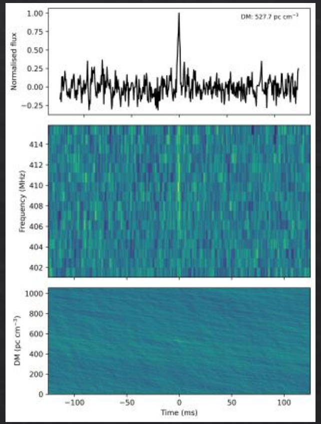

Multi-frequency campaign

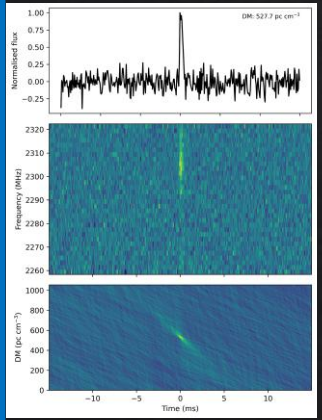

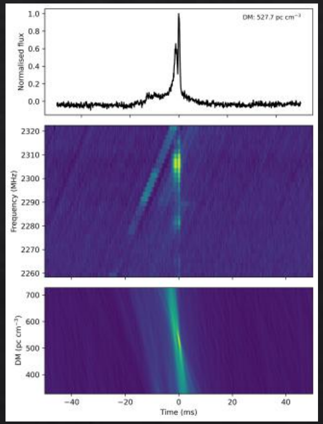

FRB 20240209A

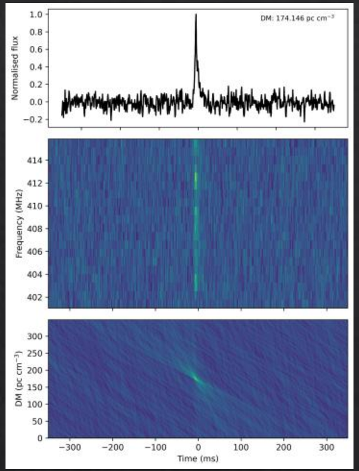

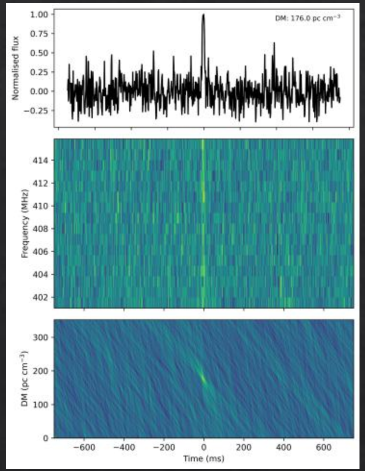

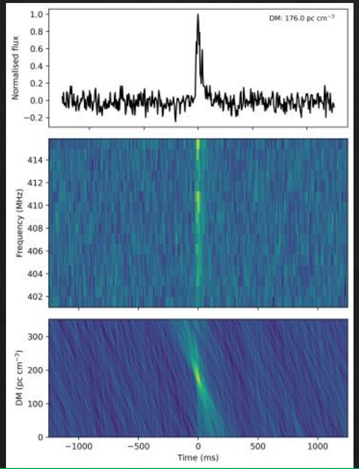

Possible $\sim$ 126 days periodicity

FRB 20240316A

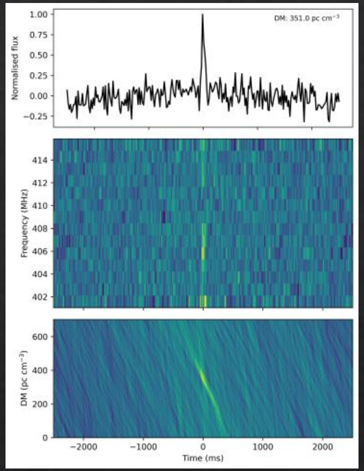

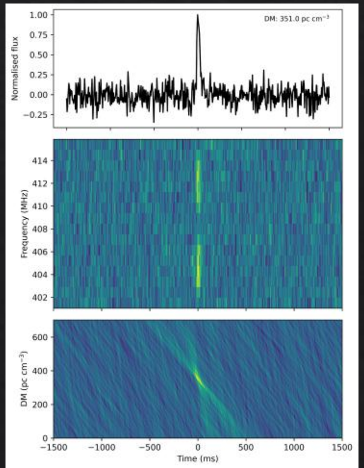

Power-law emission

Rate of detectable events $(E > E_{min})$

$$R(\lambda_{mag}, \gamma; E > E_{min,j}) = \int_{E_{min,j}}^{E_{max}} K_0 \left(\frac{E}{E_0}\right)^{-\gamma} dE$$

Rate of events with energy greater than the SGR J1935 FRB-like event $(E > E_0)$

$$\lambda_{mag} = \int_{E_0}^{E_{max}} K_0 \left(\frac{E}{E_0}\right)^{-\gamma} dE$$

Energy of the SGR J1935 FRB-like event

$$E_0 = 3 \times 10^{34}\ \text{erg}$$

Minimum detectable energy

$$E_{min,j} = 1.34 \times 10^{20} \left(\frac{\mathrm{D}}{[\mathrm{pc}]}\right) \frac{1}{G(ToA)_j}\ \text{erg}$$

Suggested maximum energy

$$E_{max} \cong 3 \times 10^{44} \left(\frac{B}{10^{16} G}\right)^2 \left(\frac{\eta}{10^{-5}}\right)\ \text{erg}$$

$$R(\lambda_{mag}, \gamma; E > E_{min,j}) = \lambda_{mag} \frac{E_{max}^{1-\gamma} - E_{min,j}^{1-\gamma}}{E_{max}^{1-\gamma} - E_0^{1-\gamma}}$$